

Magnetorheological fluids subjected to tension, compression, and oscillatory squeeze input

Ali K. El Wahed* and Loai B. Balkhoyor^a

Department of Mechanical Engineering & Mechatronics, University of Dundee, Dundee U.K.

(Received December 3, 2014, Revised April 20, 2015, Accepted April 25, 2015)

Abstract. Magnetorheological (MR) fluids are capable of changing their rheological properties under the application of external fields. When MR fluids operate in the so-called squeeze mode, in which displacement levels are limited to a few millimetres but there are large forces, they have many potential applications in vibration isolation. This paper presents an experimental and a numerical investigation of the performance of an MR fluid under tensile and compressive loads and oscillatory squeeze-flow. The performance of the fluid was found to depend dramatically on the strain direction. The shape of the stress-strain hysteresis loops was affected by the strength of the applied field, particularly when the fluid was under tensile loading. In addition, the yield force of the fluid under the oscillatory squeeze-flow mode changed almost linearly with the applied electric or magnetic field. Finally, in order to shed further light on the mechanism of the MR fluid under squeeze operation, computational fluid dynamics analyses of non-Newtonian fluid behaviour using the Bingham-plastic model were carried out. The results confirmed superior fluid performance under compressive inputs.

Keywords: magnetorheological fluids; squeeze mode; non-newtonian fluid; bingham-plastic model; tensile loads; compressive loads; oscillatory squeeze-flow

1. Introduction

Magnetorheological (MR) and electrorheological (ER) fluids are smart materials that can exhibit substantial reversible changes in their rheological properties such as yield stress when energised by magnetic and electric fields, respectively. These fluids were discovered approximately five decades ago (Winslow 1949, Rabinow 1949) and have evolved along interrelated paths. Both fluids are composed of suspensions or slurries of solid particulates, which are typically micrometers in size. Their response to an applied field is the familiar chaining of the particles in the direction of the field and the resulting “solidification” or increase in the apparent viscosity of these fluids. The dramatic and reversible field-induced rheological changes of these smart fluids permit the construction of many novel electromechanical devices that are potentially useful in the automotive, aerospace, structural, medical, and other industries (see, for example, Karakoc *et al.* 2008, Choi and Wereley 2003, Wilson and Abdullah 2010, Khanicheh *et al.* 2008).

*Corresponding author, Ph.D., E-mail: a.elwahed@dundee.ac.uk

^a Ph.D. Student, E-mail: l.balkhoyor@dundee.ac.uk

As a result, industrial applications of these fluids have seen considerable progress over the last two decades. Vibration control is considered to be the most promising area of the large-scale commercial exploitation of these fluids, which can provide controlled damping forces to meet many industrial requirements. Perhaps the most significant applications to date are the fitting of the WBI Group's magnetorheological Magniride™ and Fludicon's electrorheological eRRide™ suspension systems on commercial vehicles (Delphi Energy and Chassis Systems 2002, Johnson, 2008).

The majority of field-controllable fluids have been employed in a simple flow (El Wahed *et al.* 2002a, Sato *et al.* 2007, Nam *et al.* 2008, Nishiyama *et al.* 2011, Liao *et al.* 2012, Spaggiari and Dragoni 2012, Goldasz and Sapinski 2012) or shear mode of operation (Wang and Gordaninejad 2006, Choi *et al.* 2009, Jang *et al.* 2011, Guo *et al.* 2012, Guth *et al.* 2013, Kaluvan and Choi 2014) where the fluid is deformed in a direction orthogonal to the arrays of particulate chains. An alternative arrangement has been identified for vibration isolation (Stanway *et al.* 1992, Jolly and Carlson 1996): the squeeze mode, in which the fluid is subjected to compressive and tensile stresses in a direction parallel to the applied field. In this mode of operation, field-controllable fluids have a yield stress that is an order of magnitude higher than that in the shear or flow modes (Monkman 1995, El Wahed 2008). The characteristics of ER and MR fluids under the flow and shear modes are well understood (Farjoud *et al.* 2008). ER fluids in squeeze mode are also well-investigated (see, for example, Nakano and Nagata 2002, El Wahed *et al.* 2002b, Jung 2004, Pahlavan and Rezaeepazhand 2007, Esmonde *et al.* 2009, El Wahed 2011). However, little research has been carried out on MR fluids under the squeeze mode (El Wahed and McEwan, 2011), most of which has been directed towards rotor damping (Wang 2006, Kim *et al.* 2009, Ghaednia and Ohadi 2010, Zapomel *et al.* 2012, Hemmatian and Ohadi 2013). Furthermore, recent publications in this area involved designs of MR fluids in squeeze devices with relatively large fluid-energising coil units (Mazlan *et al.* 2008, Lin *et al.* 2013). Since squeeze mode devices are intended for short stroke damping applications, the size of these devices makes it difficult to adapt them for applications such as engine mounting. Others have focused on specific issues, such as the effects of the frequency of the magnetic field (Zhu 2007), the fluid gap size (Farjoud *et al.* 2009) and the uniformity of the magnetic field (Guo *et al.* 2013) on the performance of MR fluids under squeeze operation. Therefore, further research is required to assess the characteristics of MR fluids in squeeze mode, which could be utilised in short-stroke damping applications.

In addition, modelling field-controllable fluids is now relatively advanced (Stanway *et al.* 1996). The simplest model is the Bingham-plastic model, which is commonly used to describe the flow characteristics of MR fluids where the shear stress of the fluid is related to the rate of strain through a dimensional relationship (Maiti *et al.* 2006). The Bingham power-law or the Herschel-Bulkley model (Chooi and Oyadiji 2008) has been developed to account for the post-yield shear thinning or thickening behaviour whilst the bi-viscous model has been used to relax the rigid pre-yield behaviour (El Wahed *et al.* 2003a).

This paper presents an assessment of the comparative performance of a model MR fluid that is employed in tension, compression, and oscillatory squeeze-flow modes. Of particular interest is the effect of the strain direction on the rheological behaviour of the MR fluid, which is assessed under various mechanical and magnetic input conditions. Moreover, computational fluid dynamics (CFD) analyses employing a Bingham-plastic model were carried out to model the rheological behaviour of MR fluids under compression and tension inputs. The results confirmed the dependence of the fluid performance on the strain direction.

2. Experimental setup

2.1 Experimental facility

The experimental rig (Fig. 1) consisted of an Instron servo-hydraulic test machine (Model no. 4204) that was capable of providing a vertical oscillatory motion with a maximum force of 50 kN over speeds ranging from zero to 520 mm/min. For the precise determination of the performance of MR fluids under squeeze operation, a dedicated MR fluid cell was constructed using low-carbon steel (Fig. 2). The cross-head of the tensile machine was attached rigidly to a Kistler piezoelectric force link (Model no. 9311A) and the upper assembly (piston) of the MR fluid cell, which had a circular area, A , of approximately $7.85 \times 10^{-3} \text{ m}^2$. The lower assembly of the cell had a recessed cylindrical cavity of diameter 110 mm that formed the reservoir of the MR fluid and was rigidly attached to a second identical force link and the machine supporting frame. A toroidal electromagnetic coil was installed symmetrically about the centreline of the piston to provide the required magnetic field for the excitation of the fluid under the squeeze flow mode. The electrical excitation of the coil was achieved by a quad-mode TTI low-voltage power source (Model no. PL330QMT).

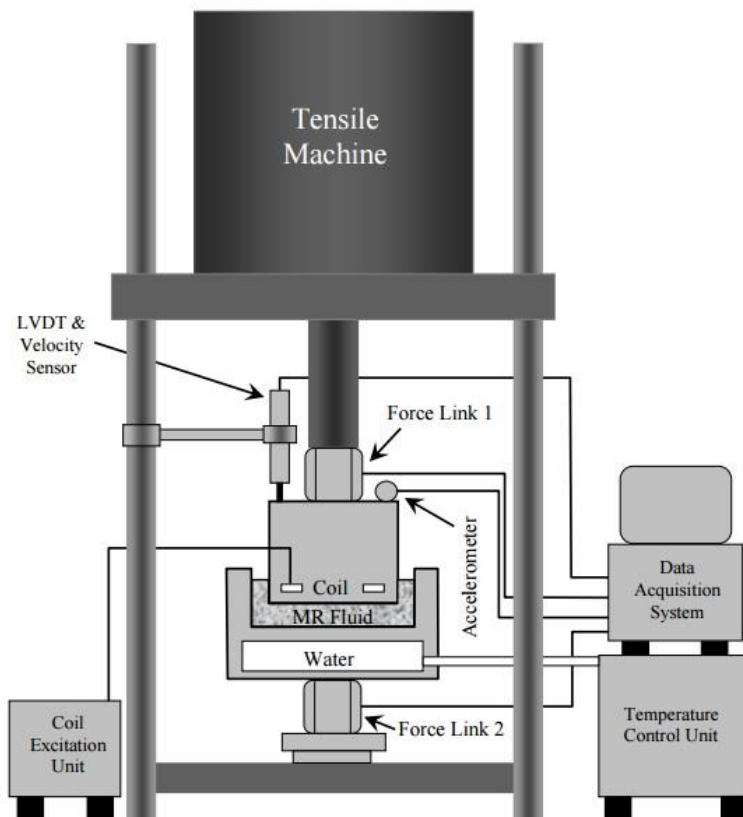


Fig. 1 Schematic of the experimental setup

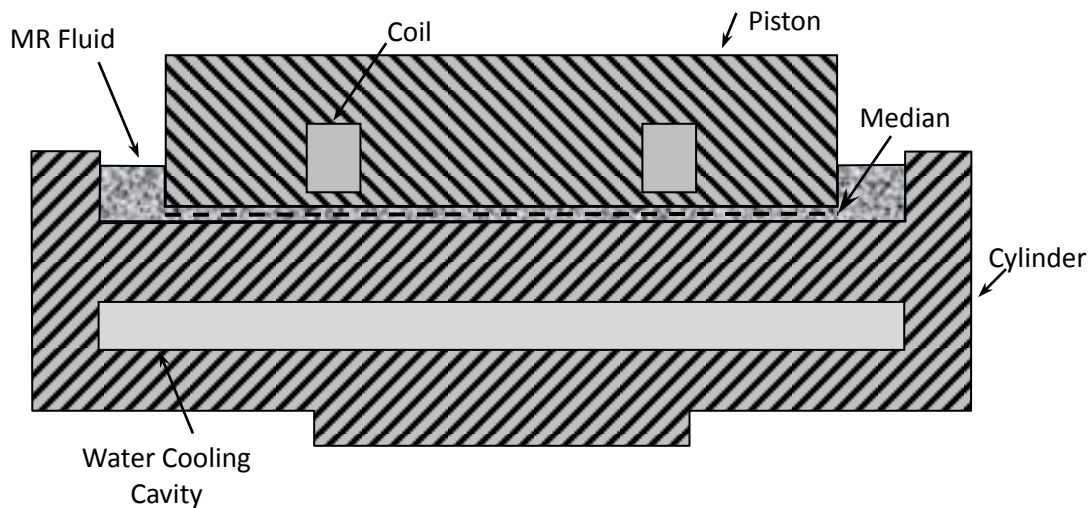


Fig. 2 Schematic of the MR fluid cell

The instantaneous displacement, velocity, and acceleration of the upper assembly were determined using an RDP LVDT (type GTX 2500), an RDP self-induced velocity sensor (Type 240A0500), and an Endevco accelerometer (Type 7254-100), respectively. Data acquisition and processing was achieved using a Measurement Group analogue-to-digital converter (Type ESAM) with a simultaneous sampling capability, which was controlled by a Pascal program running on an IBM-compatible personal computer. To allow meaningful comparisons between the results of various tests, the MR fluid temperature was maintained at a constant level by circulating water at a controlled temperature through a second closed cavity in the lower assembly using a Grant Instruments temperature controller (Model no. LTD6).

2.2 Calibration of sensors

The two force links were calibrated statically by sequential loading using small weights. A specially designed micrometer calibration unit was used to achieve an accurate calibration of the LVDT. The accelerometer was pre-calibrated by the manufacturer. It functioned as specified to within $\pm 0.6\%$ when its maximum transverse sensitivity was checked using a digital sine controller. As an additional check, the displacement signal from the LVDT was differentiated twice using central differences and the resulting signal agreed well with that from the accelerometer. Finally the data acquisition system was checked against a DC signal supplied by a millivolt calibration unit (Time Electronics Ltd., Model 404S) and was found to be accurate to within $\pm 0.5\%$.

3. MR fluid

The MR fluid used in this investigation was a suspension of carbonyl iron powder in

hydrocarbon oil produced in-house. The iron powder was supplied by Finetools SA with an average diameter of approximately $4\ \mu\text{m}$ and a density of approximately $4.3\ \text{g/cm}^3$. The kinematic viscosity of the oil at 20°C was $20 \times 10^{-6}\ \text{m}^2/\text{s}$. The weight fraction of the solid phase was approximately 80% with a magnetisation saturation in excess of 1300 kA/m.

4. Results and discussion

4.1 Experimental results

A systematic study was conducted to assess the performance of an MR fluid under tension, compression, and oscillatory squeeze-flow mode. A range of mechanical and magnetic input conditions were created using a dedicated cell that simulated a short-stroke damper. The tests consisted of the simultaneous measurement of the input force, F_i , delivered by the test machine and the transmitted force, F_t , across the fluid in addition to the displacement Δh , velocity V , and acceleration a of the upper assembly of the cell. These measurements were collected at a sampling frequency of 5 kHz for a machine input-speed of 1 mm/s. The mean separation (original gap) of the parallel plane surfaces of the MR cell, h_o , was set to 2.0 mm. The input displacement amplitude of the upper assembly was limited to 0.5 mm when the fluid was under tension or compression and to 1.0 mm (peak to peak) when the fluid was under oscillatory conditions. The magnetic field intensity across the fluid was varied based on a coil excitation current ranging from 0 to 2 A. The input displacement amplitude level was maintained throughout the test regardless of the magnetic field intensity. The fluid temperature was maintained at 20°C for all tests.

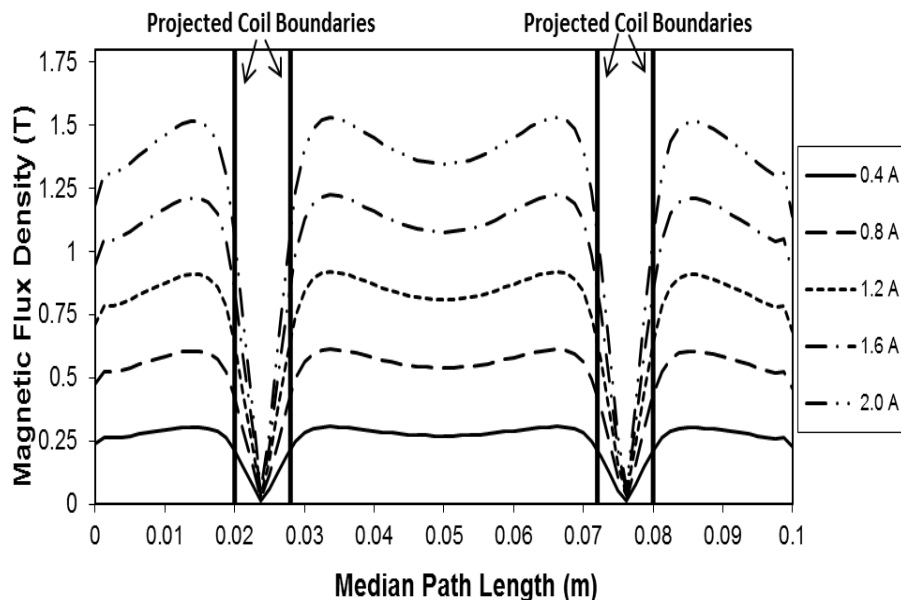


Fig. 3 Magnetic field distribution inside the MR fluid squeeze gap along the median

Electromagnetic finite element analysis (FEA) was carried out using the commercial ANSYS code to design the electromagnetic circuit of the MR fluid cell. Fig. 3 shows the variation of the magnetic flux density inside the MR fluid squeeze gap along a median path (shown in Fig. 2) for excitation currents between 0.4 and 2.0 A. The physical boundaries of the coil are superimposed onto this figure, represented by vertical solid lines. The magnetic flux density drops considerably in areas opposite the electromagnetic coil. This is due to the fact that in these locations, the magnetic flux lines do not cross the fluid gap but instead follow a short circuit around the coil. This is clearly demonstrated by the contour plot of the magnetic flux line density across the squeeze gap (shown in Fig. 4) for a coil input current of 0.4 A. Note that the flux drop occurs over less than 8% of the total magnetic field path length, which was considered to be too small to affect the magnetic circuit efficiency. This issue was also encountered in previous designs of MR fluid devices (see, for example, Blake and Gurocak 2009).

Fig. 5 shows the stress ($\sigma = F_t / A$) variation of the MR structure under a compressive loading with the strain ($\varepsilon = \Delta h / h_0$) for coil excitation currents between 0 and 2.0 A. In general, the strength of the MR viscoelastic structure increases with the coil excitation current. It can be seen that as the MR structure initially demonstrates an elastic deformation, which is represented by the linear portion of the stress-strain curve. This is followed by a plastic deformation where the stress increases with the strain, reaching a maximum value at the ultimate strength of the material before starting to decrease. This is attributed to the fact that at the early stages of the compressive loading, the MR fibrils become thicker, thus providing higher resistance to deformation up to the ultimate strength of the material. Under higher strains, they start to bend and break and consequently, the stress begins to decay. The shape of the stress-strain relationship of field-controllable fluids under compressive stress can be affected by several factors, including its strong dependence on the initial gap size (Tian *et al.* 2003). The ultimate strength of the MR structure increases with the excitation level and is reached at higher strains as the fluid becomes stronger.

The behaviour of the MR material under tensile loading is shown in Fig. 6 for the same excitation levels as for the compressive tests. Again, the MR fluid clearly demonstrates the elastic and plastic deformation regions. The stress generally increases with the excitation level. However, the MR structure is less resistant to tensile loading at higher strains when the excitation currents exceed 0.8 A. The MR fluid exhibits higher ultimate strength levels with increasing currents in general, which occur at decreasing strains.

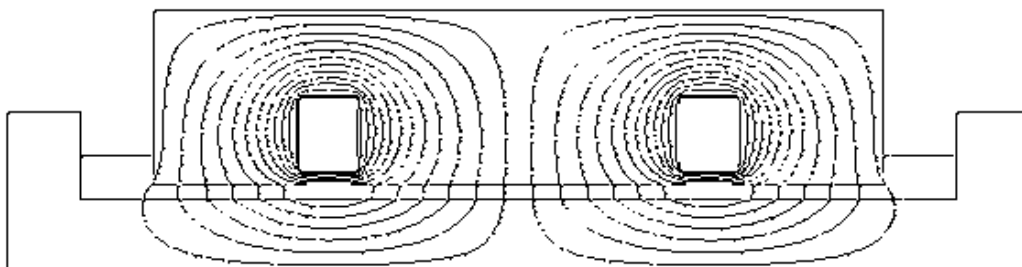


Fig. 4 Contour plot of the magnetic flux line density across the MR fluid squeeze gap

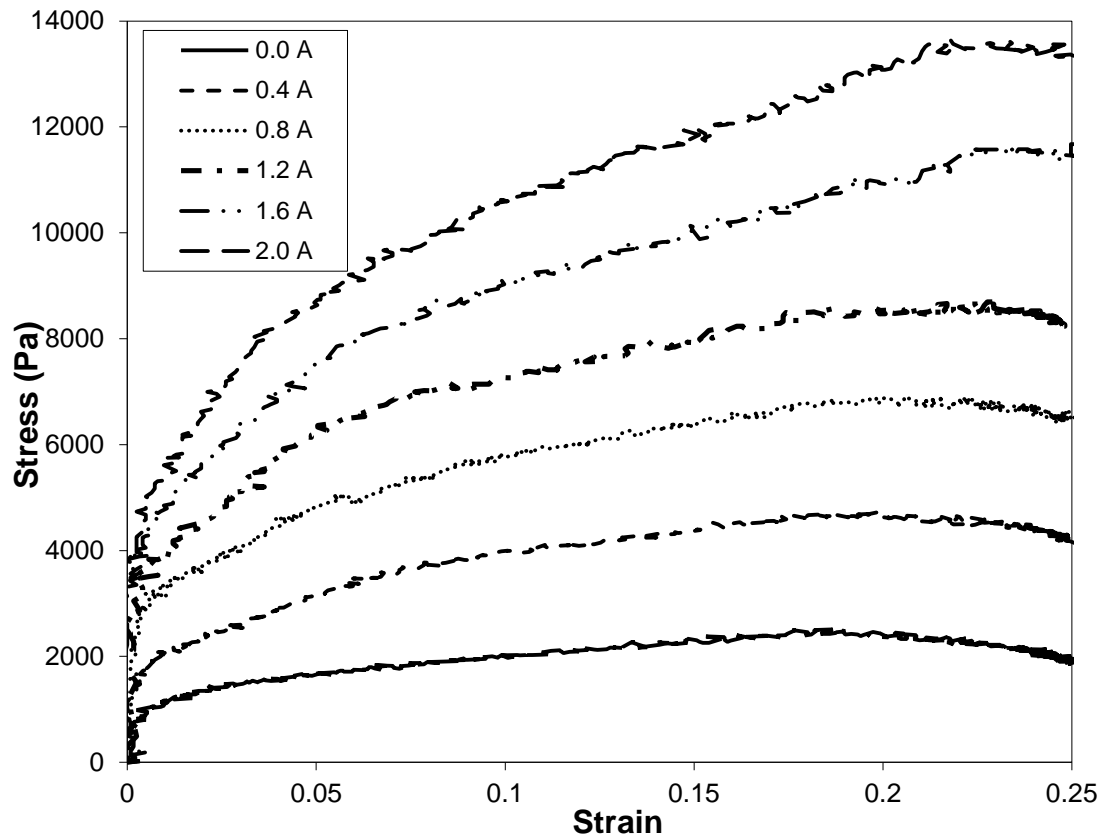


Fig. 5 Compressive stress of MR fluid versus strain

This behaviour can be attributed to the microstructure of the MR material. Greater cohesion and bond strength of the ferrous particles within the fluid fibrils are realized with greater applied currents, which provide increasing resistance to strain until the ultimate strength was reached. Thereafter, once the bonds begin to break, further bonds fail and the strain increases with decreasing stress. The stress reduction was further promoted by the fact that fluid fibrils become thinner and possibly develop necking under the conditions described above. When higher currents were applied and stronger magnetic fields established, it may be difficult for the MR fluid to enter the fluid gap from the surrounding volume during the tensile stroke. Under increasing tensile strains, it is also possible for cavitation to occur because low pressure was induced between the parallel plates. Therefore, lower tensile stresses are achieved under elevated electromagnetic fields.

Fig. 7 shows a comparison between the performance of the MR material under compressive and tensile loads for selected excitation currents. The MR structure is stronger when utilised under compression, which is demonstrated clearly within the plastic deformation region. Fig. 8 shows the influence of the coil excitation current on the ultimate strength of the MR structure, which was estimated as the peak in the stress-strain characteristics shown in Figs. 5 and 6. The ultimate

strength of the MR structure increases almost linearly with the current when the MR material was under compression, with a maximum strength of approximately 13.7 kPa when the coil was excited by a current of 2.0 A. However, the increasing maximum strength when the material was under tension peaks at 5.64 kPa at approximately 1.2 A before decreasing as the current increases further. This could be attributed to the fact that as the MR fluid underwent increasing tensile strain, stronger fibrils formed by higher magnetic field intensities may prevent fresh ferrous particles from filling the increasing volume (inner locations) between the upper and lower parallel planes of the MR fluid cell. This effect is expected to be stronger with increasing applied currents, resulting in an ultimate tensile strength of the fluid. This is unlikely to be the case when the fluid is under compressive loading since strong fibrils that form at the edge of the parallel planes may reduce the flow of the ferrous particles, which could be displaced away from the resistive area. Furthermore, when the MR fluid structure is subjected to a tensile input, the fibrils are expected to be longer and thinner which cause the reduction of their strength and subsequently their resistance to the tensile input. This is however unlikely to be the case when the fluid is subjected to a compressive input under which the fibrils are becoming shorter and wider and hence, offer larger resistance to the fluid deformation. Consequently, the ultimate strength of the fluid increases further with increasing currents.

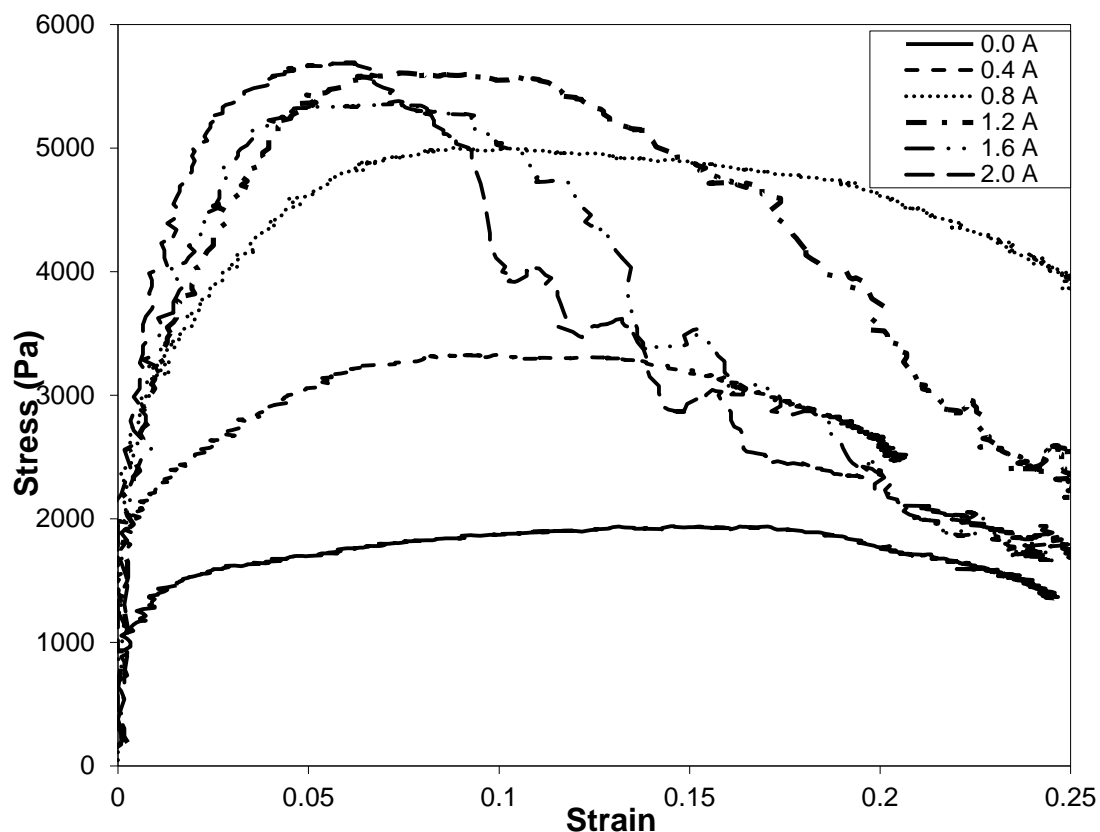


Fig. 6 Tensile stress of MR fluid versus strain

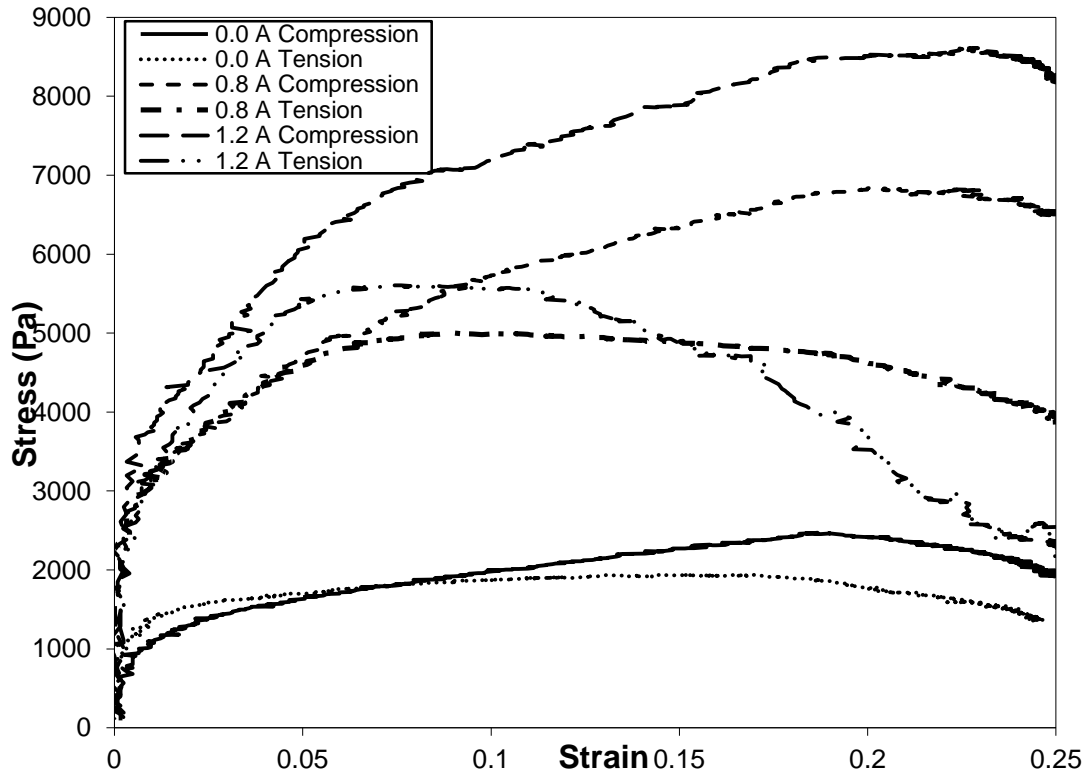


Fig. 7 Comparison between compressive and tensile stresses of MR fluid

The electric current supplied to the coil was constant while the upper assembly of the MR cell was subjected to either compressive or tensile strokes. This resulted in continuous changes in the gap size and hence, continuously variable magnetic fields across the fluid gap. Increasing the fluid gap under a tensile input results in a decreasing magnetic field strength, which is expected to cause the fluid structure to exhibit lower resistance. This effect is clearly shown in Fig. 9 where a gap increment (tensile displacement) or decrement (compressive displacement) of approximately 0.5 mm results in a 5% change in the average magnitude of the magnetic field. However, an examination of Fig. 8 indicates that this effect contributes very little to the higher MR structure performance in compression. The ultimate strength of the material under compression is higher than that in tension by approximately 20% at the lower end of the applied current range and by approximately 57% at the upper end of the range. However, the overall performance of MR structures under dynamic squeeze-flow (oscillatory) mode could be enhanced if the magnetic field is controlled based on the instantaneous squeeze gap. This ensures that the fluid is continuously subjected to a constant magnetic excitation level throughout the entire strain phase. This field control mechanism enhanced the overall performance of ER fluids in squeeze mode (El Wahed *et al.* 1998). The improved MR fluid performance under compression compared to tensile loading is also in agreement with that obtained for ER fluids (El Wahed *et al.* 2003b, Choi and Kim 2005). This is expected because ER and MR fluids share a number of characteristics.

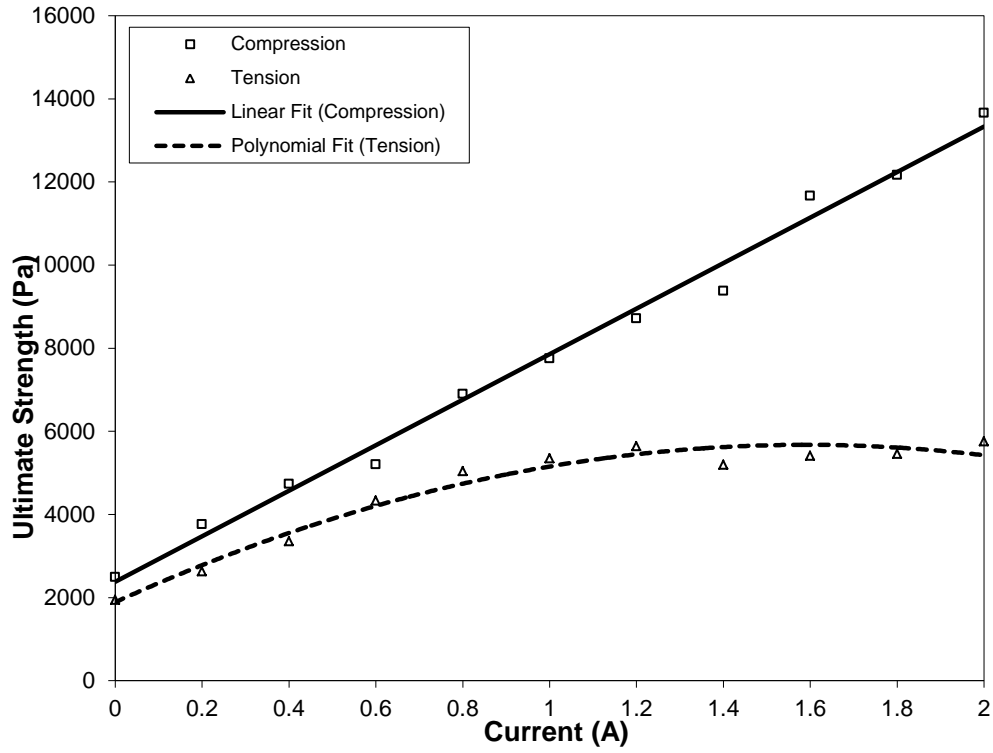


Fig. 8 Ultimate strength of MR fluid under compressive and tensile loading

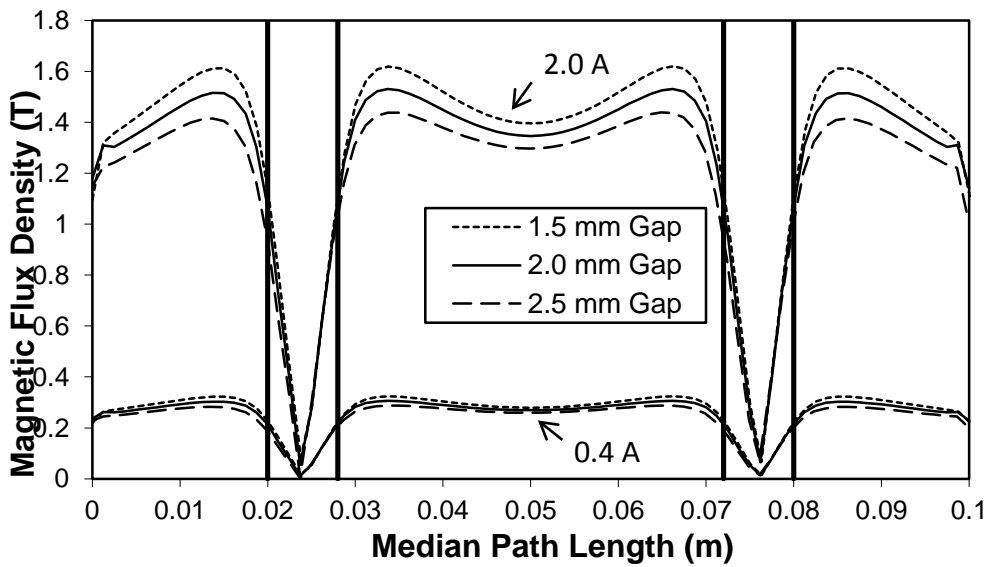


Fig. 9 Effects of the MR fluid gap on the magnetic flux density

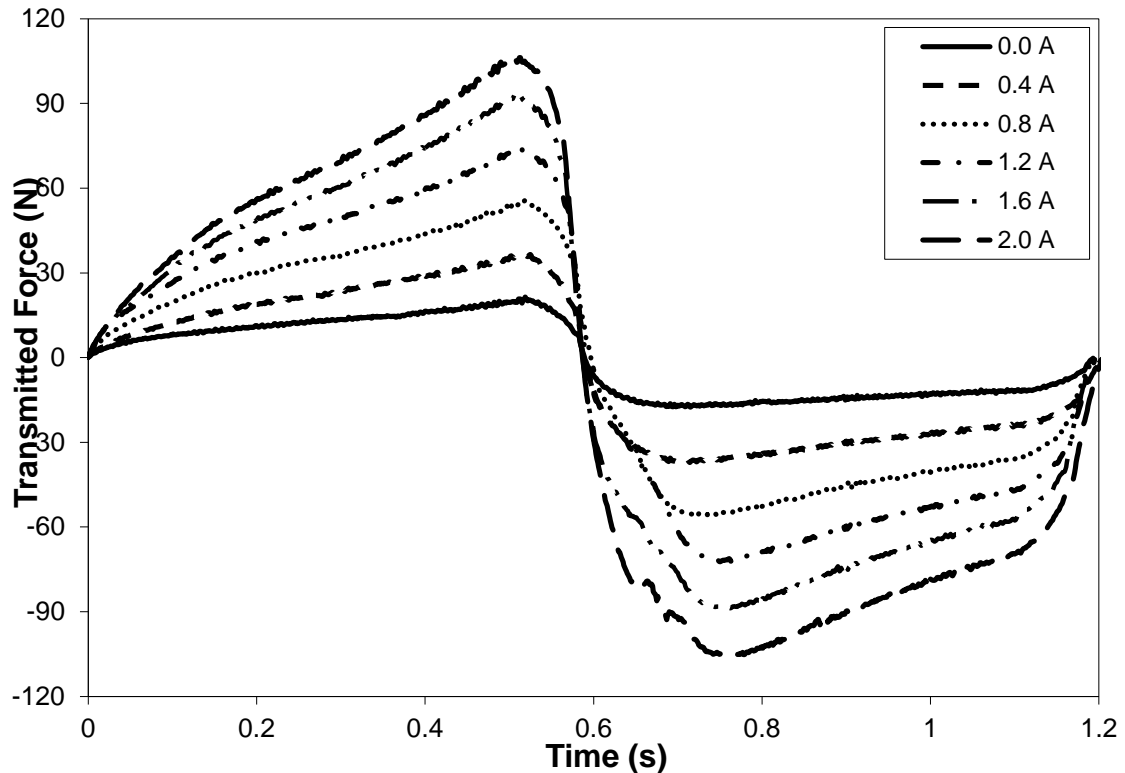


Fig. 10 Variation of transmitted force with time for the MR fluid under oscillatory squeeze-flow mode

The performance of the MR fluid in dynamic (oscillatory) squeeze-flow mode is shown in Fig. 10 where the variation of the transmitted force with time is shown for currents ranging between 0.0 A and 2.0 A for input displacements of ± 0.5 mm. As the coil excitation current is increased and the magnetic field becomes stronger, the fluid transmits higher forces. The tensile loading machine attempts to overcome the increasing resistance of the fluid by supplying higher input forces in order to maintain the same level of the input displacement. The variations of the transmitted force with displacement and velocity are shown in Figs. 11 and 12, respectively, for the same applied current range. The shape of these hysteresis curves is likely influenced by the inherent nonlinearity of MR fluids, which is associated in the current short-stroke application and a large percentage of the squeeze cycle. The whirl orbits, Fig. 11, are plotted over approximately one cycle and illustrate the change in the level of the transmitted force due to the development of higher yield stresses with increasing field strength. The amount of damping is represented by the energy dissipated by the MR cell over one vibration cycle and is given by the area enclosed by the force-displacement loops. This area, and hence, the damping capacity of the cell increases with increasing magnetic field strengths. Both the force-displacement and force-velocity figures show the clear difference between the compression and tension phases of each cycle. The fluid performance during the compression phase is represented by the right-hand half of the loops. The performance is enhanced over the compression phase compared to the tension phase (left half of the loops).

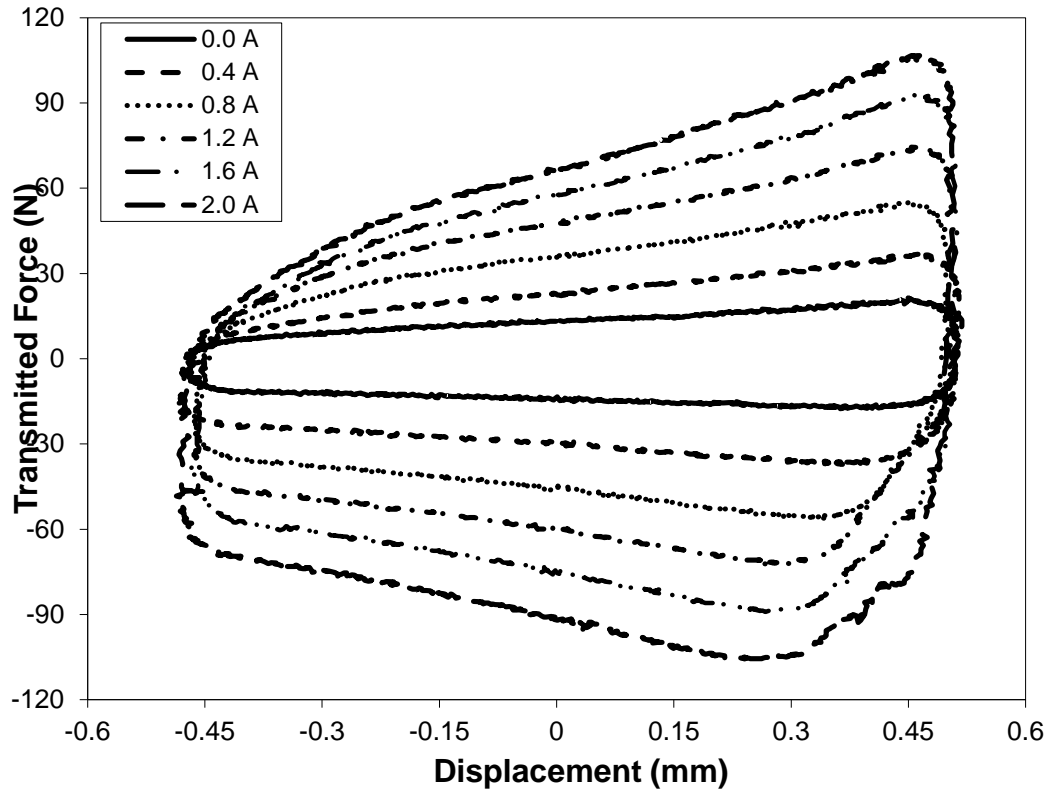


Fig. 11 Variation of transmitted force with displacement for the MR fluid under oscillatory squeeze-flow mode

This fluid performance is in agreement with that predicted theoretically and experimentally for ER fluids (El Wahed *et al.* 2003a, Choi and Kim 2005) and corresponds to the behaviour of Bingham-plastics that combine the yield properties of solids with the Newtonian flow properties of fluids. Moreover, the force-velocity hysteresis cycles in Fig. 12 reach maximum values, which when projected back to the force axis, may result in the yield force values (Pang *et al.* 1997). The yield forces also increase with increasing applied currents, as shown in Fig. 13.

4.2 ANSYS results

The commercial ANSYS code is widely utilised in CFD analysis to simulate the flow of Newtonian fluids in complex devices. It is well documented that such analysis would become more complex if the fluid is non-Newtonian (Brunn and Abu-Jdayil 2007, Rufai and Ayeni, 2010). In this investigation, the ANSYS FLOTTRAN CFD code was used to study the complex flow of an excited MR fluid that is squeezed between the driven piston and the stationary cylinder of the MR fluid cell. An intermediate gap of 2.0 mm was assumed from which the piston was allowed to travel either upward or downward to simulate the tensile and compressive phases, depending on whether the piston velocity is positive or negative, respectively.

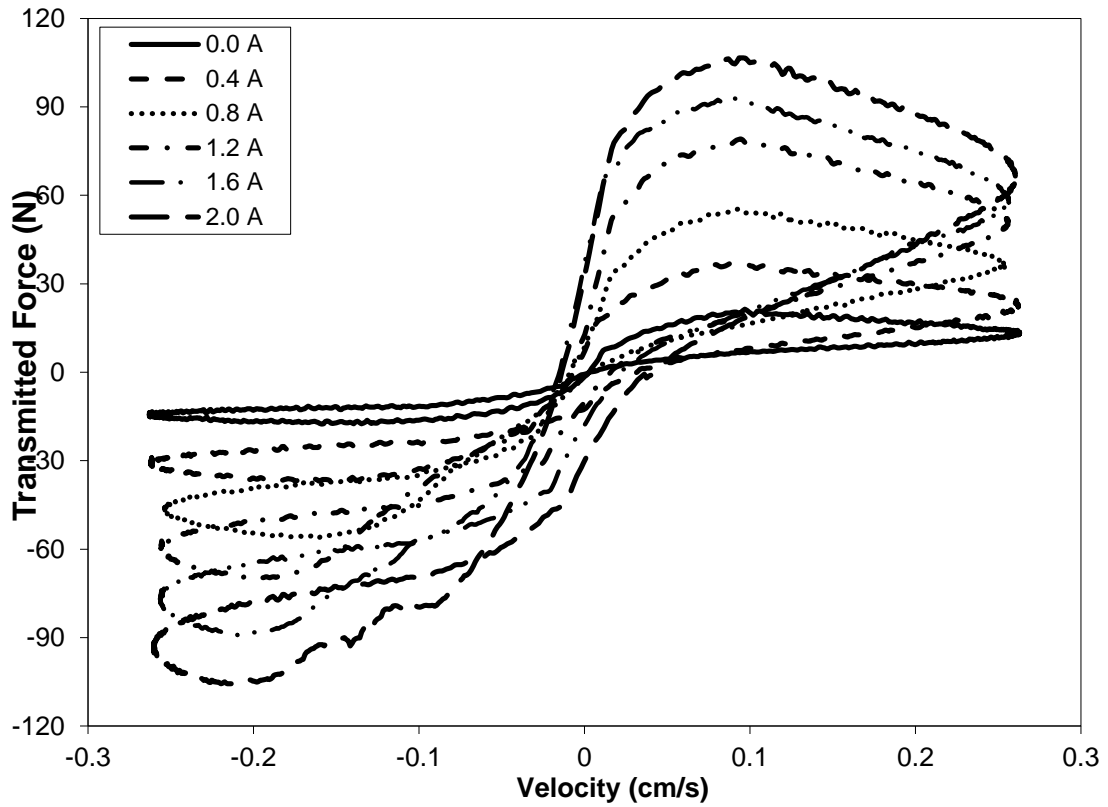


Fig. 12 Variation of transmitted force with velocity for the MR fluid under oscillatory squeeze-flow mode

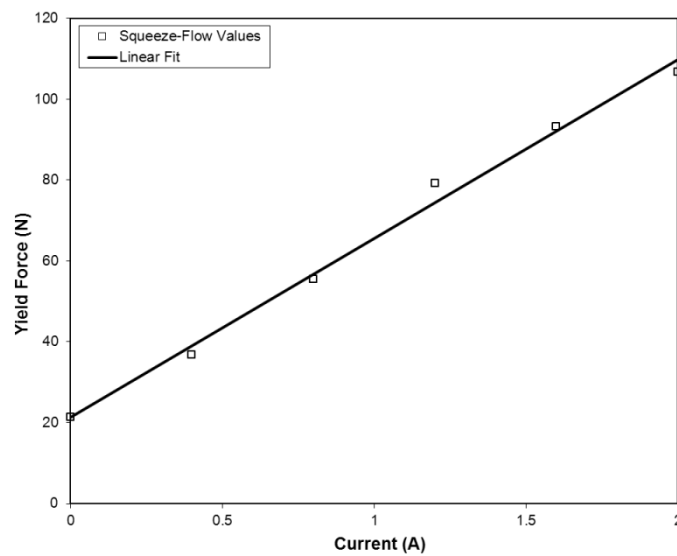


Fig. 13 Variation of yield force with current for the MR fluid under oscillatory squeeze-flow mode

An input displacement of 0.5 mm was specified, which resulted in final fluid gaps of 1.5 mm (in compression) or 2.5 mm (in tension). Two-dimensional fluid models similar in dimensions to either the compressed or tensioned fluid domains were set up in ANSYS. Fig. 14 shows the fluid model used for the compression analysis. Analysing the piston displacement (LVDT) data for a compression stroke in which the MR fluid gap was reduced from 2 mm to 1.5 mm, it is clear that although the input velocity of the Instron machine was set at a certain level, the actual piston velocity was not constant throughout the entire stroke. This is due to the fact that piston accelerates and decelerates at the beginning and end of the stroke, respectively. This is also the case when the fluid is under tensile input. A steady state can be assumed to model the part of the stroke where the displacement increased linearly with time, i.e., during a constant velocity period. In this investigation, and in order to obtain meaningful analysis results, this constant velocity was approximated to be equivalent to the tensile machine velocity, which was set at 1.0 mm/s. The fluid model was then meshed using a mapped mesh technique to generate two-dimensional quadrangular elements with an element edge length of 0.1 mm. A magnified portion of the mesh is shown in Fig. 15. The boundary conditions of the model are shown in Fig. 16. The fluid was driven by the moving piston with a velocity that was equivalent to the tensile machine velocity. Fluid flow calculations were conducted for the Lord MRF132DG magnetorheological fluid. The physical properties required for the CFD simulations are readily available: the plastic viscosity was 0.092 Pa.s at 20°C, the density was 3.09 g/cm³, and yield strength of the fluid was 42kPa at approximately 0.75 T (Aachen 2010). In addition, the fluid was assumed to be incompressible and the Bingham-plastic model was employed to account for the non-Newtonian behaviour of the MR fluid. The Bingham-plastic model was available from the CFD package and is given by Eq. (1)

$$\tau = \eta \dot{\gamma} + \tau_y (H) \quad (1)$$

where η , τ , $\dot{\gamma}$, τ_y , and H are the fluid viscosity, shear stress, shear rate, fluid dynamic yield stress, and magnetic field intensity, H , respectively.

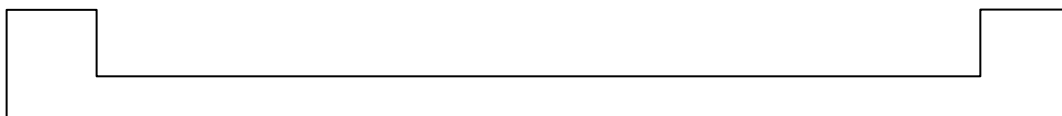


Fig. 14 MR fluid cell model for ANSYS analysis

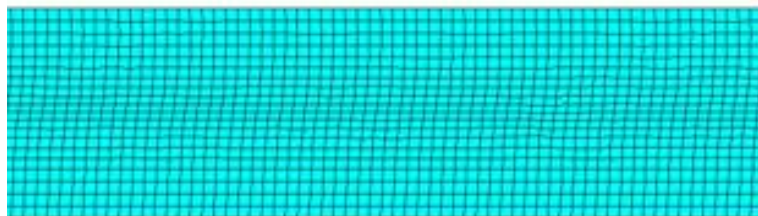


Fig. 15 Finite element mesh distribution within a section of the MR fluid gap

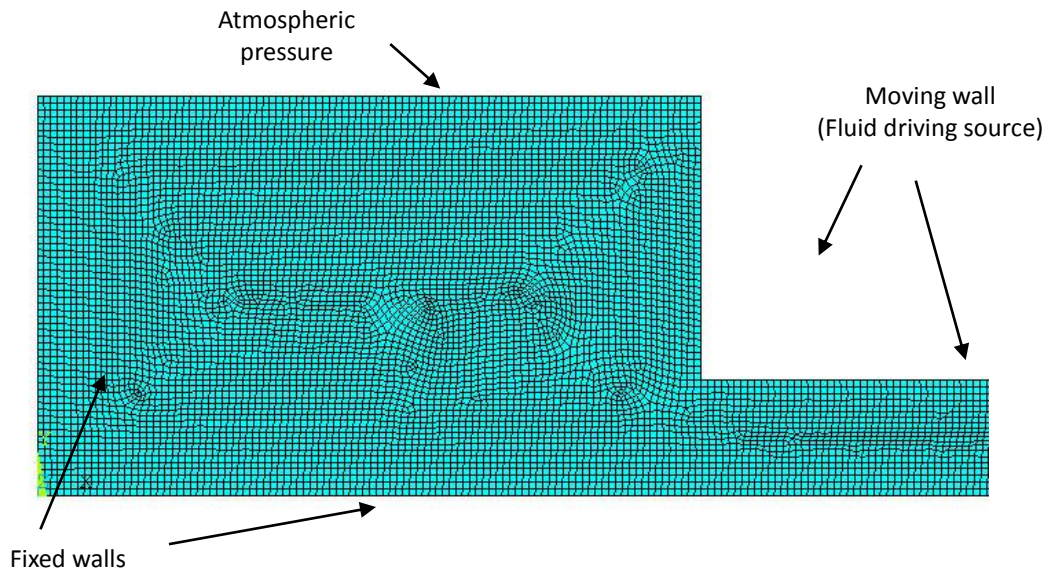


Fig. 16 Part of the meshed model under specific loading conditions

The models were solved and the results are first presented in terms of velocity contour plots for the case when the fluid is under compressive input Fig. 17(a). The fluid velocity is close to zero in areas around the cell centre and reaches a maximum close to the edge of the cell piston Fig. 17(b). Similar analyses were repeated for an MR cell under tensile input. The tension model was very similar to the compression model; however, the velocity of the piston was upwards. This allowed the MR fluid to enter the parallel fluid gap from the surrounding cylindrical fluid volume.

Fluid velocity profiles were calculated by performing path plots across the fluid gap at various radial distances from the centre of the cell. Fig. 18 shows the velocity profiles for both loading modes at two cell radial positions, 10 mm and 40 mm, which represent a point midway between the centre of the piston and the coil and a point midway between the coil and the outer edge of the cell piston, respectively. This Fig. clearly shows the difference between the two velocity profiles at the two radii, which confirms an increasing fluid velocity from the cell centre towards the edge of the cell. However, the tension model shows smaller maximum velocities in comparison with those acquired from the compression model for the same radii (0.605 cm/s compared to 0.886 cm/s at 1 cm and 2.212 cm/s compared to 3.48 cm/s at 4 cm). This indicates that the fluid flow velocity under tensile operation is equivalent to 65-70% of the compression velocity. The difference in these velocities was therefore considered to be an additional consideration factor in the comparison between the compression and tension operations of MR fluids. Also, the flow velocity in areas away from the cell centre was considerably high in both the compression and tension models compared to the velocity of the driving piston. This indicates that the flow of the MR fluid within the squeeze gap would have a substantial influence on the performance of the fluid under squeeze

operation. Furthermore, the velocity profiles are fully parabolic for the compression mode, indicating regions of complete post-yield behaviour (Lange *et al.* 2001). The broadness of the velocity profiles for the tension mode indicates a pre-yield region, which appears to be more pronounced towards the centre of the cell (smaller radii). This would suggest that the tension mode induces less stress than compression as the fluid yield stress was not reached across the full gap of the fluid. This may explain why the experimental performance of the fluid (Figs. 7 and 8) was better under compressive rather than tensile loading.

5. Conclusions

This paper presented an assessment of the comparative performance of MR fluids in vibration isolation under tension, compression, and oscillatory squeeze-flow modes. The fluid exhibited higher strengths when utilised under compression. In particular, the fluid ultimate strength under compression loading was higher than that of a fluid under tensile loading by approximately 20% to 57% depending on the applied current range. The fluid under oscillatory squeeze-flow mode had a higher damping capacity with increasing applied currents, which was also dependent on the strain direction.

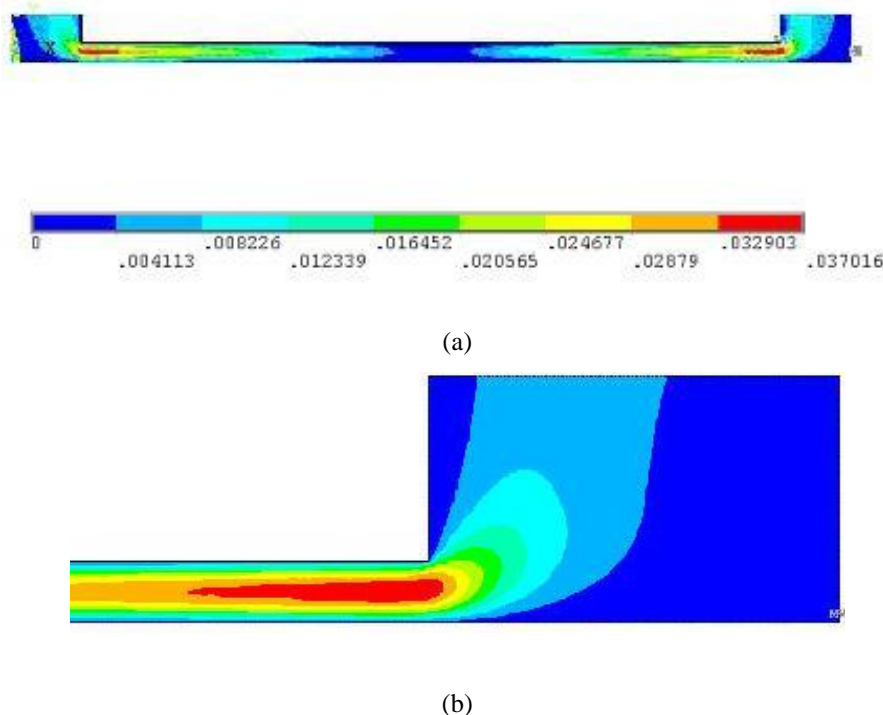


Fig. 17 (a) Velocity contour plot for the MR fluid under compressive loading (velocities are in m/s) and (b) A magnified portion of the velocity contour plot for the MR fluid under compressive loading

CFD analyses were carried out to assess the MR fluid performance under compressive and tensile operations, and the Bingham-plastic model was employed to model the MR fluid behaviour under high magnetic fields. The CFD analyses confirmed that the lower fluid strength under tension could be mainly attributed to the presence of pre-yield pockets, reducing its overall resistance. The CFD modelling itself has proven to be useful to understanding the behaviour of the MR squeeze film and may be used in the future to achieve device designs and assessments for specific engineering applications.

The squeeze film MR cell represents a short-stroke damping device that requires a minimal fluid volume to create large forces and highly controllable authority. A particularly attractive feature of the controllable squeeze film device is its simplicity and compactness.

Acknowledgments

This research did not receive any specific grant from any funding agency in the public, commercial, or not-for-profit sectors.

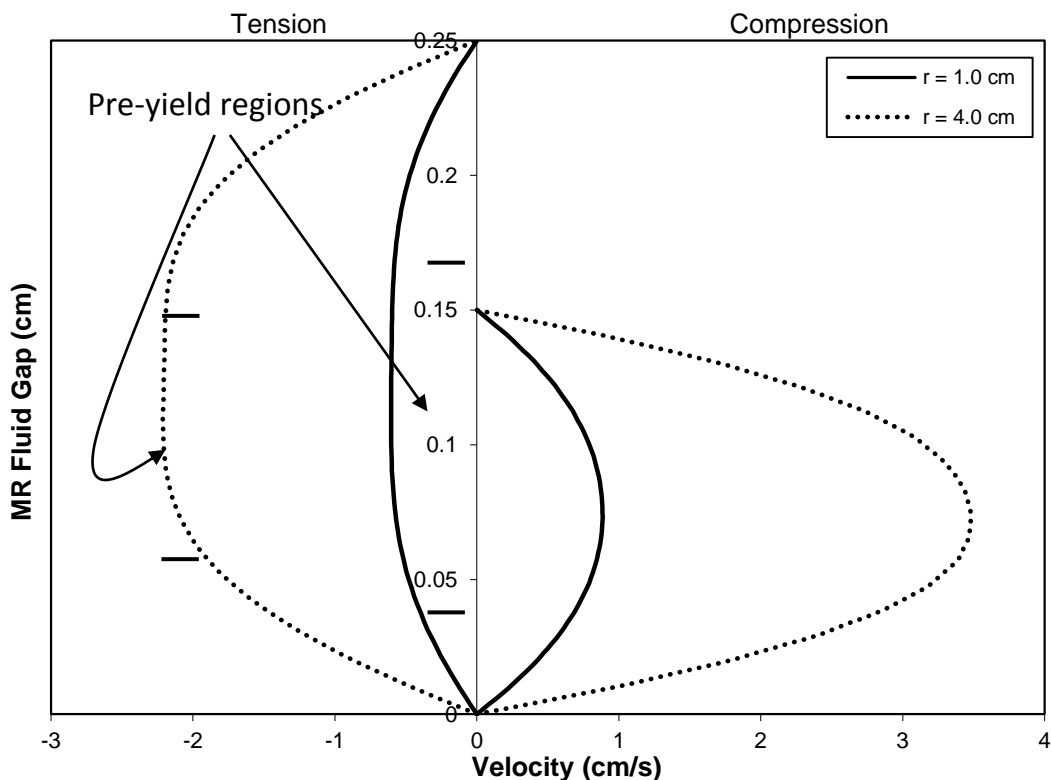


Fig. 18 Flow velocity profiles inside the MR fluid gap (compression and tension modes for two radii)

References

- Aachen, A. (2010), *Lord Corporation Business Development Manager Europe*, Lord MR fluids technical summary, Private Communication.
- Blake, J. and Gurocak, H.B. (2009), "Haptic glove with MR brakes for virtual reality", *Trans. Mechatron.*, **14**(5), 606-615.
- Brunn, P.O. and Abu-Jdayil, B. (2007), "Axial annular flow of plastic fluids: dead zones and plug-free flow", *Rheol. Acta.*, **46**(4), 449-454.
- Choi, Y.T. and Wereley, N.M. (2003), "Vibration control of a landing gear system featuring electrorheological/magnetorheological fluids", *J. Aircraft*, **40**(3), 432-439.
- Choi, S.B. and Kim, K.S. (2005), "Tensile and compressive behaviours of smart electrorheological materials", *Key Eng. Mater.*, **297-300**, 646-652.
- Choi, B.H., Nam, Y.J., Yamane, R. and Park, M.K., (2009), "Effect of cluster formation on dynamic response of an electrorheological fluid in shear flow", *Proceedings of the 11th Conference on Electrorheological Fluids and Magnetorheological Suspensions*, Journal of Physics: Conference Series 149 (2009) 012004.
- Chooi, W.W. and Oyadiji, S.O. (2008), "Design, modelling and testing of magnetorheological (MR) dampers using analytical flow solutions", *Comput. Struct.*, **86**(3-5), 473-482.
- Delphi Energy & Chassis Systems (2002), Pub. DE-00-E-019.
- El Wahed, A.K., Sproston, J.L. and Stanway, R. (1998), "The performance of an electrorheological fluid in dynamic squeeze flow under constant voltage and constant field", *J. Phys. D: Appl. Phys.*, **31**, 2964-2674.
- El Wahed, A.K., Sproston, J.L. and Schleyer, G.K. (2002a), "Electrorheological and magnetorheological fluids in blast resistant design applications", *Mater. Design*, **23**(4), 391-404.
- El Wahed, A.K., Sproston, J.L. and Stanway, R. (2002b), "The rheological characteristics of electrorheological fluids in dynamic squeeze", *J. Intell. Mat. Syst. Str.*, **13**(10), 655-660.
- El Wahed, A.K., Stanway, R. and Sproston, J.L. (2003a), "The influence of mechanical input amplitude on the dynamic response of an electrorheological fluid in squeeze flow", *Int. J. Vehicle Des.*, **33**(1-3), 153-170.
- El Wahed, A.K., Sproston, J.L. and Stanway, R. (2003b), "An improved model of ER fluids in squeeze-flow through model updating of the estimated yield stress", *J. Sound Vib.*, **268**(3), 581-599.
- El Wahed, A.K. (2008), "Performance evaluation of electrorheological fluids under mixed shear and squeeze mode", *Proceedings of the 11th Int. Conf. New Actuators*, Bremen, Germany.
- El Wahed, A.K. (2011), "The influence of solid-phase concentration on the performance of electrorheological fluids in dynamic squeeze flow", *Mater. Design*, **32**(3), 1420-1426.
- El Wahed, A.K. and McEwan, C.A. (2011), "Design and performance evaluation of magnetorheological fluids under single and mixed modes", *J. Intell. Mat. Syst. Str.*, **22**(7), 631-643.
- Esmonde, H., See, H. and Swain, M.V. (2009), "Modelling of ER squeeze films at low amplitude oscillations", *J. Non-Newtonian Fluid Mech.*, **161**(1-3), 101-108.
- Farjoud, A., Vahdati, N. and Yap Fook, F. (2008), "MR-fluid yield surface determination in disc-type MR rotary brakes", *Smart Mater. Struct.*, **17**(3), 1-8.
- Farjoud, A., Cavey, R., Ahmadian, M. and Craft, M. (2009), "Magneto-rheological fluid behavior in squeeze mode", *Smart Mater. Struct.*, **18**(9), 1-8.
- Ghaednia, H. and Ohadi, A. (2010), "Effect of thermal growth on vibration behavior of flexible rotor system mounted on MR squeeze film damper", *Proceedings of the ASME 2010 10th Biennial Conference on Engineering Systems Design and Analysis*, paper ESDA2010-24864.
- Goldasz, J. and Sapinski, B. (2012), "Nondimensional characterization of flow-mode magnetorheological/electrorheological fluid dampers", *J. Intell. Mat. Syst. Str.*, **23**(14), 1545-1562.
- Guo, C., Gong, X., Xuan, S., Zong, L. and Peng, C. (2012), "Normal forces of magnetorheological fluids under oscillatory shear", *J. Magn. Magn. Mater.*, **324**(6), 1218-1224.
- Guo, C., Gong, X., Xuan, S., Yan, Q. and Ruan, X. (2013), "Squeeze behavior of magnetorheological fluids under constant volume and uniform magnetic field", *Smart Mater. Struct.*, **22**, 045020, (7pp).

- Guth, D., Wiebe, A. and Maas, J. (2013), "Design of shear gaps for high-speed and high-load MRF brakes and clutches", *Proceedings of the 13th Int. Conf. on Electrorheological Fluids and Magnetorheological Suspensions (ERMR2012)*, Journal of Physics: Conference Series, **412** (2013) 012046.
- Hemmatian, M. and Ohadi, A. (2013), "Sliding mode control of flexible rotor based on estimated model of magnetorheological squeeze film damper", *J. Vib. Acoust.*, **135**(5), 051023 (11 pages).
- Jang, K.I., Min, B.K. and Seok, J. (2011), "A behavior model of a magnetorheological fluid in direct shear mode", *J. Magn. Magn. Mater.*, **323**(10), 1324-1329.
- Johnson, L. (2008), "Electrorheological dampers for industrial and mobile applications – an overview of design variations, product realisation and performance", *Proceedings of the 11th Int. Conf. New Actuators*, Bremen, Germany.
- Jolly, M.R. and Carlson, J.D. (1996), "Controllable squeeze film damping using magnetorheological fluid", *Proceedings of the 5th Int. Conf. New Actuators*, Bremen, Germany.
- Jung, W.J., Jeong, W.B., Hong, S.R. and Choi, S.B. (2004), "Vibration control of a flexible beam structure using squeeze-mode ER mount", *J. Sound Vib.*, **273**(1-2), 185-199.
- Karakoc, K., Park, E.J. and Suleman, A. (2008), "Design considerations for an automotive magnetorheological brake", *Mechatron.*, **18**(8), 434-447.
- Kaluvan, S. and Choi, S.B. (2014), "Design of current sensor using a magnetorheological fluid in shear mode", *Smart Mater. Struct.*, **23**, 127003 (7pp).
- Khanicheh, A., Mintzopoulos, D., Weinberg, B., Tzika, A.A. and Mavroidis, C. (2008), "Evaluation of electrorheological fluid dampers for applications at 3-T MRI environment", *Trans. Mechatron.*, **13**(3), 286-294.
- Kim, K.J., Lee, C.W. and Koo, J.H. (2009), "Optimal positioning and control of a MR-squeeze film damper for reducing unbalanced vibrations in a rotor system with multiple masses", *J. Vib. Acoust.*, **131**(4), paper 041006.
- Lange, U., Richter, L. and Zipser, L. (2001), "Flow of magnetorheological fluids", *J. Intell. Mat. Syst. Str.*, **12**(3), 161-164.
- Li, W.H., Du, H., Chen, G. and Yeo, S.H. (2001), "Viscoelastic properties of MR fluids under oscillatory shear", *Proceedings of the SPIE 4331*, Smart Structures and Materials 2001: Damping and Isolation, Newport Beach, CA, USA.
- Liao, C.R., Zhao, D.X., Xie, L. and Liu, Q. (2012), "A design methodology for a magnetorheological fluid damper based on a multi-stage radial flow mode", *Smart Mater. Struct.*, **21**, 085005 (12pp).
- Lin, C., Yau, H., Lee, C. and Tung, K. (2013), "System identification and semiactive control of a squeeze-mode magnetorheological damper", *IEEE/ASME T. Mechatronics*, **18**, 6, 1691.
- Maiti, D.K., Shyju, P.P. and Vijayaraju, K. (2006), "Vibration control of mechanical systems using semi-active MR-damper", *Smart Struct. Syst.*, **2**(1), 61-80.
- Mazlan, S.A., Ekreem, N.B. and Olabi, A.G. (2008), "Apparent stress-strain relationships in experimental equipment where magnetorheological fluids operate under compression mode", *J. Phys. D: Appl. Phys.*, **41**(9), 095002.
- Monkman, G. (1995), "The electrorheological effect under compressive stress", *J. Phys. D: Appl. Phys.*, **28**(3), 588-593.
- Nakano, M. and Nagata, T. (2002), "ER properties and flow-induced microstructures of an ER fluid between two parallel disk electrodes in squeeze flow mode", *Int. J. Modern Phys. B*, **16**(17-18), 2555-2561.
- Nam, Y.J., Park, M.K. and Yamane, R. (2008), "Dynamic responses of electrorheological fluid in steady pressure flow", *Exp. Fluids*, **44**(6), 915-926.
- Nishiyama, H., Takana, H., Shinohara, K., Mizuki, K., Katagiri, K. and Ohta, M. (2011), "Experimental analysis on MR fluid channel flow dynamics with complex fluidwall interactions", *J. Magn. Magn. Mater.*, **323**(10), 1293-1297.
- Pahlavan, L. and Rezaeepazhand, J. (2007), "Dynamic response analysis and vibration control of a cantilever beam with a squeeze-mode electrorheological damper", *Smart Mater. Struct.*, **16**(6), 2183-2189.
- Pang, L., Kamath, J.M. and Wereley, N.M. (1997), "Analysis and testing of a linear stroke magnetorheological damper", AIAA/ASME Adaptive Structures Forum, Long Beach, CA, USA, paper no.

- AIAA 98-2040.
- Rabinow, J. (1949), "The magnetic fluid clutch", *AIEE Trans.*, **67**, 1308-1315.
- Rufai, O.R. and Ayeni, R.O. (2010), "Non-Newtonian fluid flow between parallel plates", *Proceedings of the 10th Int Congress Fluid Dyn.*, Ain Soukhna, Egypt.
- Sato, Y., Shiraishi, T. and Morishita, S. (2007), "Design of magnetorheological devices based on flow modes", *Int. J. Appl. Electromagn. M.*, **25**, 607-611.
- Spaggiari, A. and Dragoni, E. (2012), "Effect of pressure on the flow properties of magnetorheological fluids", *J. Fluids Eng.*, **134**(9), 091103-1 to 091103-9.
- Stanway, R., Sproston, J.L., Prendergast, M.J., Case, J.R. and Wilne, C.E. (1992), "ER fluids in the squeeze-flow mode: an application to vibration isolation", *J. Electrostat.*, **28**(1), 89-94.
- Stanway, R., Sproston, J.L. and El Wahed, A.K. (1996), "Applications of electrorheological fluids in vibration control: a survey", *Smart Mater. Struct.*, **5**(4), 464-482.
- Tian, Y., Wen, S. and Meng, Y. (2003), "Compressions of electrorheological fluids under different initial gap distances", *Phys. Rev. E*, **67**(5), 051501.
- Wang, X. and Gordaninejad, F. (2006), "Study of magnetorheological fluids at high shear rates", *Rheologica Acta*, **45**, 899-908.
- Wang, J., Feng, N., Meng, G. and Hanh, E.J. (2006), "Vibration control of rotor by squeeze film damper with magnetorheological fluid", *J. Intell. Mat. Syst. Str.*, **17**(4), 353-357.
- Wilson, C.M.D. and Abdullah, M.M. (2010), "Structural vibration reduction using self-tuning fuzzy control of magnetorheological dampers", *Bull. Earthq. Eng.*, **8**(4), 1037-1054.
- Winslow, W.M. (1949), "Induced fibrillation of suspensions", *J. Appl. Phys.*, **20**, 1137-1140.
- Zapomel, J., Ferfecki, P. and Forte, P. (2012), "A computational investigation of the transient response of an unbalanced rigid rotor flexibly supported and damped by short magnetorheological squeeze film dampers", *Smart Mater. Struct.*, **21**(10), 105011.
- Zhu, C. (2007), "Controllability of a magnetorheological fluid squeeze film damper under sinusoidal magnetic field", *Key Eng. Mater.*, **334-335**, 1089-1092.